Diels-Alder-Chitosan based dissociative covalent adaptable networks

Camille Chapelle, Baptiste Quienne, Céline Bonneaud, Ghislain David, Sylvain Caillol

Diels-Alder-Chitosan based dissociative covalent adaptable networks

Camille Chapelle[1], Baptiste Quienne[1], Céline Bonneaud[1], Ghislain David[1*], Sylvain Caillol[1]

[1] ICGM, Univ Montpellier, CNRS, ENSCM, Montpellier, France

Abstract

Four different films were prepared from chitosan modified with furfuryl glycidyl ether (FG) by Diels Alder reaction with different maleimide-based cross linker. At first, a preliminary study led to structural identification and better understanding of the reaction. For the first time, Diels-Alder and retro Diels-Alder reactions were evidenced by NMR spectroscopy and DSC on chitosan based systems. Then, chitosan of 30,000 g/mol and 150,000 g/mol were modified by FG with 20% substitution degree (DS). The resulting products were then cross-linked with bis and trimaleimide cross-linkers to produce films possessing interesting mechanical properties. For the first time for chitosan-based films, DMA measurement highlighted retro Diels-Alder between 110 and 130°C. Film also showed interesting hydrophobicity and fat absorption. They also exhibited resistance in acidic media whereas crude chitosan films were destroyed.

Keywords

Chitosan-based films, Diels-Alder crosslinking, thermoresponsive materials, trimaleimide

Highlights

- Synthesis of *N*-(furfuryl glycidyl) chitosan was simple and carried out in one step
- *N*-(furfuryl glycidyl) chitosan based films were produced by Diels-Alder crosslinking reactions with bis and trimaleimide moieties
- Retro Diels-Alder reaction was highlighted in chitosan based films
- Thermoresponsive films from chitosan can be designed to produce novel materials

1. Introduction

Natural polysaccharides such as gelatin, hyaluronic acid, guar gum or chitosan are currently widely used due to their renewable and biodegradable nature (Dragan & Dinu, 2019),

(Hamedi et al., 2018)' (Pakdel & Peighambardoust, 2018). They are extensively used in biomedical and pharmaceutical applications as their non-toxicity combined with a good biocompatibility make them suitable in these fields. Among them, chitosan shows attractive properties with a low cost and availability. Chitosan comes from the deacetylation of chitin which is extracted from various natural resources like shrimp shells, squids, insects or mushrooms. It is a cationic polysaccharide made of β-D-glucosamine and N-acetyl-β-D-glucosamine units linked by a glyosidic bond (1→4). This polysaccharide is characterized by its source, its acetylation degree (DA) and its molar mass. Chitosan possesses two hydroxyl and one amino groups per glucosamine unit allowing its functionalization. More specifically, the amino group is responsible for the intrinsic properties of the chitosan chains and, thanks to its nucleophilic character, allows the introduction of new functionalities (Gregorio Crini , Pierre-Marie Badot, n.d.).

Chitosan was already described as a film-forming polymer on its own (S. Bhuvaneshwari *, D.Sruthi*, V. Sivasubramanian*, 2014)' (Elsabee & Abdou, 2013), or mixed with other polymers or fibers. (Liu et al., 2017)' (Y.X. Xua, K.M. Kimb, M.A. Hannaa,∗, 2005)' (Kaya et al., 2018) Crosslinked chitosan films are generally obtained by reaction with glutaraldehyde, diepoxides, dianhydride, genipin and tripolyphosphate (Divya Nataraj, Seema Sakkara, 2018)' (Jin et al., 2004)' (Singh, Kuldeep Rajat Suri & Rana, 2012)' (Tiwary & Rana, 2010)' (Kavianinia et al., 2014) and few literature is provided on Diels-Alder based hydrogels for chitosan but not in view of film forming.(Matsumoto et al., 2016)' (Montiel-Herrera et al., 2015)' (Montiel et al., 2015)' (Elschner et al., 2018) In 2015, Montiel-Herrera *et al.* (Montiel-Herrera et al., 2015) synthesized Diels-Alder chitosan microparticles. They functionalized chitosan with furan chitosan by a two-step reductive amidation (**Erreur ! Source du renvoi introuvable.** b)). Indeed, furfural was reacted first with the amines to form the corresponding Schiff base followed by its reduction. In their work, microspheres were synthesized by using a

bismaleimide having three ethylene glycol units and chitosan with an average molar mass of 130,000 g/mol. The mixture of furan and maleimide compounds was added dropwise into vegetable oil at 65 °C creating the microspheres by ensuring a continuous and efficient stirring. Finally, the microspheres demonstrated low swelling abilities with the different mixtures employed but the release of methylene blue was assessed. Later, Garcia-Astrain *et al.*(García-astrain et al., n.d.) followed the same procedure but they employed gold nanoparticles covalently bonded to maleimide functionalities. The same team also carried out studies with different maleimide cross-linkers: either a maleimide functionalized chitosan to afford fully chitosan-based hydrogels (Guaresti et al., 2017) or a poly(ethylene oxide) and poly(propylene oxide)-based bis maleimide [21, 22]. Finally, supramolecular hydrogels were fabricated by using a bismaleimide containing cyclodextrins in its backbone (Zhang et al., 2018). In any of those cases, all teams used a chitosan substituted via reductive amidation as previously mentioned. Even though, the Diels-Alder reaction was highlighted using UV-vis and IR studies, no deeper investigation has been performed on the reaction mechanisms. Going further, retro Diels-Alder has never been revealed for chitosan-based compounds even if its use has been recognized for many applications such as self-healing of various polymers (Gandini et al., 2018) (Vauthier et al., 2019) (Yang et al., 2020).

Hence, this present study is dedicated for the first time to the synthesis and characterization of dissociative covalent adaptable networks of chitosan by Diels-Alder chemistry. In this work, furan groups were grafted onto chitosan in one step with furfuryl glcidy ether to avoid the use of boric reducing agents. The furan functionalized chitosan furan was then able to react with maleimide by Diels-Alder reaction. This methodology was thoroughly applied to chitosan oligomers (M_w=1,800 g/mol) and also to chitosan of higher molar masses i.e. M_w =30,000 g/mol and 150 000 g/mol. The work on shorter chains allowed elucidating the Diels-Alder reaction mechanism, using a maleimide model, under different

reaction conditions by ^{1}H NMR spectroscopy. After this first step of optimization, the Diels-Alder and retro Diels-Alder reactions were highlighted for the first time on chitosan systems by infrared spectroscopy (FT-IR), ^{1}H NMR and differential scanning calorimetry (DSC) on a model reaction between monomaleimide and 30,000 g/mol chitosan. Afterwards, the higher molar masses polysaccharides were tested in the presence of ethylene oxide and propylene oxide-based maleimide cross-linkers, including a trimaleimide, having different degrees of functionality to create films. Both Diels-Alder and retro Diels-Alder were deeply investigated on the films by dynamic mechanical analysis (DMA) in comparison with previous studies where no proof other than FT-IR for DA, of the occurrence for both reactions was brought so far. The influence of the chitosan length as well as the cross-linkers nature was studied, water capacity measurements at different pHs and contact angle determination were performed to evaluate some of the film properties.

2. Materials & Methods

2.1. Materials

Maleic anhydride, zinc chloride were purchased from Sigma Aldrich. Furfuryl glycidyl ether, Jeffamine EDR-148, chloroform and hexamethyldisilizane were respectively purchased from Acros Organics, Huntsman Corporation, VWR chemicals and ABCR. The monomaleimide (MI) PEO (n=19) PPO (m=3) were provided by Specific Polymers. Chitosan with DA around 10-15% CH30 (Mw 30,000 g/mol), CH150 (Mw 150,000 g/mol) were purchased from Glentham Science. Acetic acid (AcOH), sodium acetate (NaAc), sodium nitrite ($NaNO_2$), lithium bromide (LiBr), sodium azide (NaN_3), sodium hydroxide (NaOH), hydrochloric acid (HCl), acetone (>98%) were purchased from Sigma and used without purification, HPLC water (>99%) was purchased from VWR.

2.1. Synthesis of chitosan oligomers functionalised with furfuryl glycidyl ether (FGO)

The depolymerization of 30,000 g/mol chitosan was performed by nitrous deamination involving $NaNO_2$ as previously described (Chapelle et al., 2019). Briefly, 1g (w/w) of chitosan was dissolved in 90 mL of AcOH (350µL in 90 mL of deionized water) solution overnight (pH 4.5). Once solubilized, a freshly prepared solution (10 mL) containing 0.4 eq (164 mg) of $NaNO_2/NH_2$ was added to the solution. The solution was stirred at 50°C for 3 h. The solutions were then freeze dried for 24 h and the lyophilisates were dried under vacuum for 24 h to obtain chitosan oligomers.

1 g of the obtained oligomers were solubilised in 20 mL of DMSO and 1 eq (818 µL) of furfuryl glycidyl ether was added. After 24 h stirring at 60°C, the product was precipitated in cold acetone, centrifugated and dried to obtain a hydroscopic orange powder.

^{1}H NMR (400 MHz, D_2O, 25 °C, δ): δ 8.2-8.5 (s, $H_{aldehydes}$), 8-7.1 (H_{imines}), 7.4 (s, Hα), 6.4 (d, 12 Hz, 1H Hβ, 1H Hγ), 5.0 (d, 5 Hz, 1H $H_{1\ gemdiol}$), 3.2-4.4 (m, 1H $H_{2\ acetyl}$, 1H H_3, 1H H_4, 1H H_5, 2H H_6), 2.5 (m, 1H, H_2), 2.0 (s, 3H, H_{CH3}), 4.8 (s, HOD).

2.2. General procedure for the synthesis of furan chitosan via epoxy-amine reaction

1g of CH30 and CH150 were solubilised in 100 mL of deionised water and 1 eq (818 µL) and 1.2 eq (981 µL) respectively of furfuryl glycidyl ether was added in 10 mL of DMSO. After 24h stirring at 60°C, the product was precipitated by addition of a 1M NaOH solution. The product was then centrifugated and washed with acetone and several time with deionised water until neutral pH. The product was finally freeze dried during 12h. Substitution degree (DS) of FGCH30 and FGCH150 were measured by ^{1}H NMR (400 MHz, D_2O, 25 °C, δ): 7.6 (s, Hα), 6.5 (d, 12 Hz, 1H Hβ, 1H Hγ), 3.5-4.1 (m, 1H $H_{2\ acetyl}$, 1H H_3, 1H H_4, 1H H_5, 2H H_6), 3.2 (m, 1H, H_2), 2.0 (s, 3H, H_{CH3}), 4.7 (s, HOD).

2.3. Synthesis of furfuryl chitosan grafted with monomaleimide

1g of FGCH30 was solubilized in 100 mL of 1% acetic acid solution. 1 eq of MI/FG was added in 10 mL of DMSO and the solution was stirred at 65 °C for 24 h. The product was precipitated in cold acetone, centrifuged and washed with acetone to get rid of unreacted MI. A yellow powder was obtained after drying the product under vacuum for 6 h.

^{1}H NMR (400 MHz, D_2O, 25 °C, δ) 7.6 (s, Hα), 6.5 (d, 12 Hz, 1H Hβ, 1H Hγ), 6.3-6.7 (m, 1H Hυ, 1H Hʎ), 3.5-4.1 (m, 1H $H_{2\ acetyl}$, 1H H_3, 1H H_4, 1H H_5, 2H H_6) 3.5 (s, nH $H_{PEO/PEG}$), 3.2 (m, 1H, H_2), 2.0 (s, 3H, H_{CH3}), 1.1 (s, 2H H_{CH2}), 4.8 (s, HOD).

2.4. General procedure for the synthesis of bismaleimide or Synthesis of BMI and TMI

Maleic anhydride (2.5 eq) was solubilized in chloroform and Jeffamine EDR-148 or Jeffamine T-403 in chloroform was added dropwise. The reaction mixture was left to stir overnight. Then $ZnCl_2$ (2.5 eq) was added at R.T. and the mixture was heated at 40 °C. Finally HMDS (2.5 eq) was added dropwise and the reaction mixture was allowed to heat at 85 °C during 5 h. The reaction was stopped. Silica gel was poured and the reaction mixture was filtrated. A liquid-liquid extraction was performed with D.I. water and the organic phase was washed with D.I. water (*3) and dried with $MgSO_4$. The solvent was then evaporated to afford white crystals (yield=62 %).

^{1}H NMR (400 MHz, $CDCl_3$, 25 °C, δ) BMI: 6.70 (s, 4H, H_a), 3.7 (td, 4H, H_c, α-azote, $^3J_{H\text{-}H}$ = 5.7 Hz), 3.6 (td, 4H, H_d, β-azote, $^3J_{H\text{-}H}$ = 5.7 Hz), 3.55 (s, 4H, H_e)

^{1}H NMR (400 MHz, $CDCl_3$, 25 °C, δ) TMI: 6.63 (s, 6H, H_a), 4.31 (m, 3H, H_b, α-azote), 3.0-3.85 (m, 21H, H_b, H_d, H_e), 1.3-1.32 (dd, 9H, H_c, β-azote), 0.95-1.08 (m, 6.5H, H_c, H_f), 0.5-0.84 (m, H_g)

2.5. General procedure for the Film formation

Films of chitosan were prepared as followed: CH30 and CH150 were dissolved in 2% acetic acid solution at 1wt% and 0.5wt% concentration respectively. 1 eq of maleimide per furan

units was added in 250 µL of DMSO and the solution was homogenized using a speed mixer for 3 min at 2500 rpm. 1mL of the prepared solution was deposed on a Teflon sheet and heated in the oven at 65°C for 12h. Control films were realised with the same procedure by adding 250 µL of DMSO to the chitosan solution before going into the oven.

2.6. Nuclear Magnetic Resonance (NMR) spectroscopy

NMR spectra were recorded on a Bruker AVANCE III 400MHz spectrometer instruments using TopSpin 3.5 operating at 400.13 (^{1}H) and100.62 (^{13}C) MHz at room temperature except if specified. D_2O and $CDCl_3$ were used as internal references. The letters s, d, t, q, quint, sext and spt stand for singlet, doublet, triplet, quartet, quintuplet, sextet and septuplet respectively.

2.7. Fourier Transform Infrared Spectroscopy (FTIR)

Spectra were recorded on a Nicolet 210 Fourier transform infrared spectroscopy (FTIR) spectrometer. The characteristic IR absorptions mentioned in the text are reported in cm^{-1}. Materials analyses were recorded using an ATR accessory. Three replicates were made for films analysis to check their homogeneity.

2.8. Differential Scanning Calorimetry (DSC)

Analyses were carried out using a NETZSCH DSC200F3 calorimeter. Constant calibration was performed using indium, *n*-octadecane and *n*-octane standards. Nitrogen was used as purge gas. Approximately 10 mg of sample were placed in perforated aluminum pans and the thermal properties were recorded between -35 °C and 190 °C at 10 °C/min to observe the enthalpy of reaction. All the reported temperatures are mean values.

2.9. Contact angle (CA)

Contact angles were measured on a Dataphysics Contact angle System OCA Apparatus coupled with SCA20 software. Briefly, a 3 µl drop of water or hexadecane was placed on the film, picture was captured and the angle was measured. The operation was reproduced 3 times for each solvent and each film.

2.10. Swelling ratio (SWR)

Three samples of around 20 mg each were separately put in PBS pH 7.4 0.1 M and acidic water (2 % acetic acid). At selected time intervals after immersion, the samples were removed, the excess of liquid was withdrawn with paper and the samples were weighed before being put in back to their solution. The swelling ratio was calculated using the Equation 2 where m_2 is the mass of the material after swelling in water and m_1 is the initial mass of the material.

$$SWR = \frac{m_2 - m_1}{m_1} \times 100 \qquad \textit{Equation 2}$$

2.11. Dynamic mechanical analysis

Dynamic mechanical analyses (DMA) were carried out on Metravib DMA 25 with Dynatest 6.8 software. Samples were tested according to uniaxial tension mode while heating at a rate of 3 °C/min from -80 °C to + 180 °C, at a frequency of 1 Hz with a fixed strain of 10^{-5} m. These conditions have been chosen to study the elastic behavior of the materials.

3. Results and Discussion

3.1. Synthesis of maleimides

The synthesis of maleimides was carried out following common procedures. The ring-opening of maleic anhydride was performed using Jeffamine-type amines overnight at room temperature in chloroform. Two starting amines were employed: Jeffamine EDR-148 containing two ethylene oxide units and two primary amines and Jeffamine T-403 containing 5-6 propylene oxide units and three primary amines. By addition of zinc chloride and hexamethyldisilizane, the ring-closure was completed after 5 h at 85 °C. After purification, the final maleimides were obtained in correct yields and called BMI for the bismaleimide from Jeffamine EDR-148 (Figure *1* b)) and TMI for the trismaleimide from Jeffamine T-403 (Figure *1* a)).

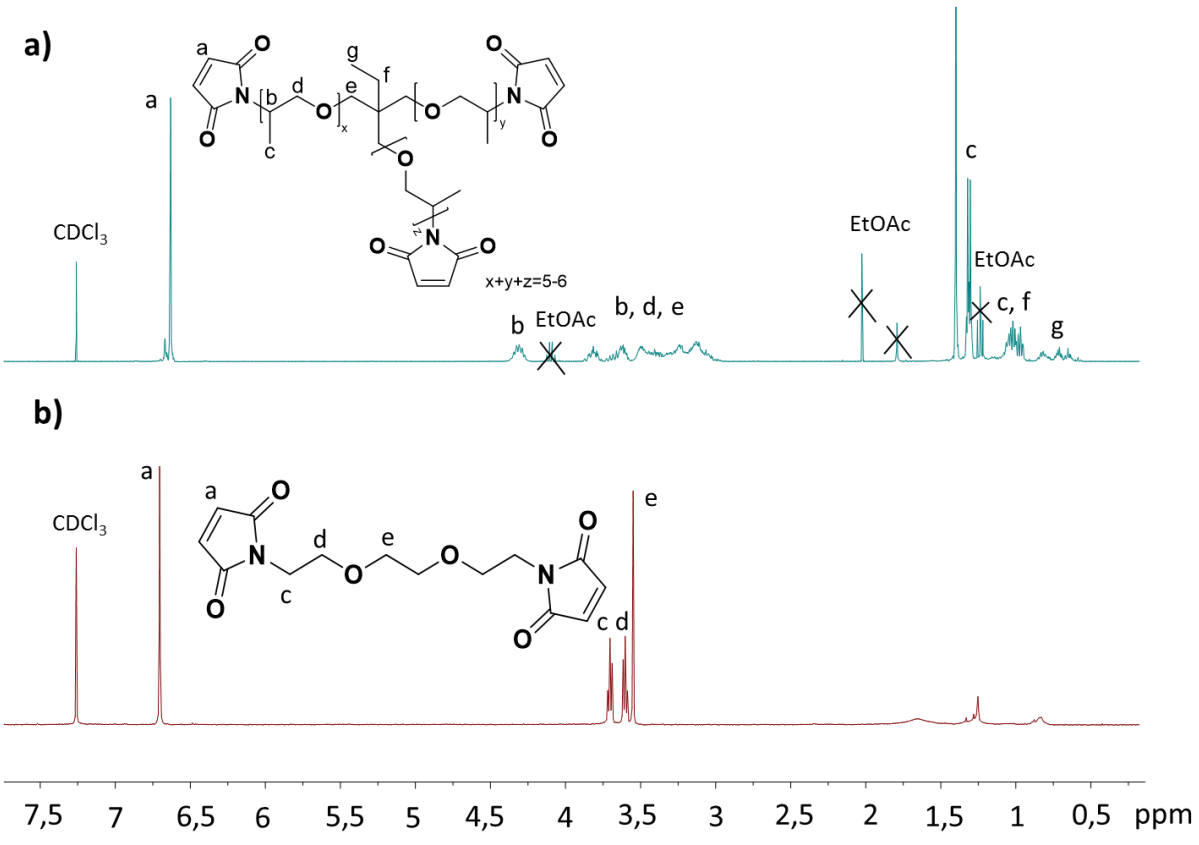

Figure 1. a) ^{1}H NMR spectrum of TMI b) ^{1}H NMR spectrum of BMI

3.2. Synthesis of furan-based chitosan compounds: oligosaccharides and polysaccharides

Epoxy amine reactions are often used for chitosan functionalisation. Reaction involving furfuryl glycidyl ether (FGE) and carboxymethyl chitosan has been described by Na et al.(Na et al., 2012), who confirmed that the reaction occurred on the free amines that are more nucleophiles than alcohol groups of chitosan in the reaction condition (aqueous solution pH 11, 60°C, 48 h). This simple reaction was a one step-procedure as opposed to previous works using furfural and boric reducing agents to perform reductive amination(Montiel-Herrera et al., 2015)' (Guaresti et al., 2018) (**Erreur ! Source du renvoi introuvable.** b)).

FGE was covalently linked to free amine groups on chitosan and oligochitosan, as indicated from both FT-IR (SI 1) and ^{1}H NMR spectra (*Figure 3* b)). The ^{1}H NMR spectrum showed the expected chemical shifts generated by protons bonded to furan rings at 6.3 and 7.4 ppm. The substitution degrees (DS) were calculated using the signal of the acetylated unit of chitosan at 2.0 ppm (which represents 16% of the macromolecule) compared to furan signals integrating for the three protons of the furan group (α). The DS calculation was done differently in comparison to a previous method (Montiel-Herrera et al., 2015) which used the proton in α-position of the free amine (Glc) of chitosan as a reference. However, the chemical shift of the α-proton is dependent on the DS. Thus, it could not be used as a reference as its position changed because of the chemical modification. The acetyl signal (GlAc) at 2.0 ppm was consequently chosen as a reliable reference and the DS was calculated following the equation (1).

$$DS = \frac{I\alpha}{I\alpha + IGlc + \frac{1}{3}IGlAc} \quad Equation\ (1)$$

Three different chitosan-based starting reagents were employed. An oligomer resulting from the depolymerisation of chitosan was firstly obtained with a final molar mass of approximatively 1,800 g/mol. Two molar masses for chitosan products were also used: 30,000

and 150,000 g/mol standing for CH30 and CH150. The three final furan-based products were respectively called FGO, CH30FG and CH150FG from the oligomer, the chitosan of 30 and 150,000 g/mol respectively. It was proved that the higher the molar masses, the lower the DS for the same amount of FGE used. This is why the number of equivalent was increased for longer chains to obtain similar DS independently of the starting chitosan CH30 or CH150, i.e 1.2 eq for CH30FG and 1.5 eq for CH150FG. The DS were respectively 40% for FGO, 25% for both CH30FG and CH150FG. Finally, the furan addition was also confirmed by IR spectroscopy with the signal at 730 cm^{-1} corresponding to the furan ring (SI 1)

3.3. Preliminary studies by NMR on the reactivity of furan-based chitosan with maleimide (MI)

3.3.1. Influence of the solvent

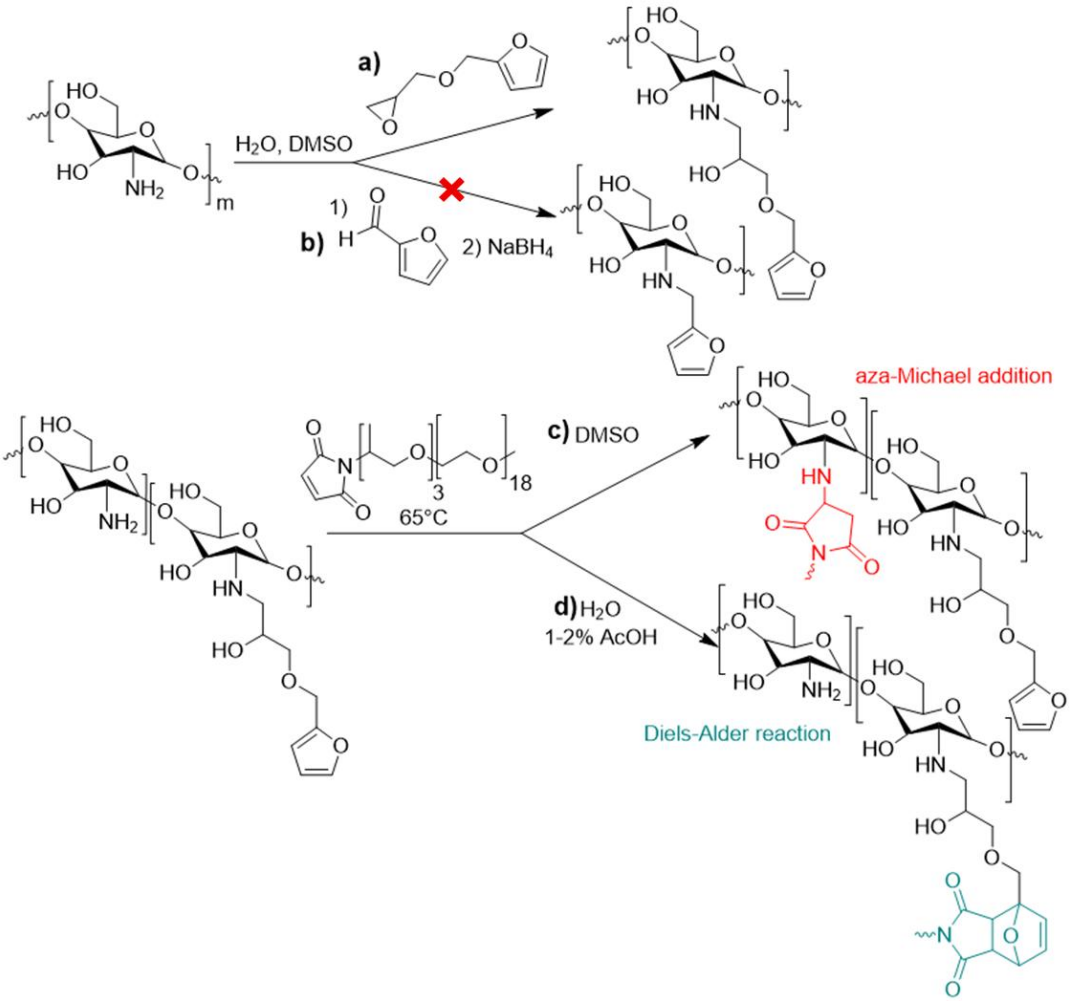

Scheme 1. Functionalization of chitosan with a) furfural in two steps (Montiel-Herrera et al., 2015) b) FGE in one step and reaction between chitosan and MI in c) DMSO d) H_2O with 1 or 2 % AcOH

In order to determine the working conditions, a model study was carried out. This model reaction was performed between chitosan oligomer FGO and a monomaleimide MI possessing ethylene oxide and propylene oxide units and was monitored by ^{1}H NMR. Firstly, the reaction was carried out in DMSO at 65 °C, to solubilize both chitosan oligomers and MI. It was shown that the reaction started in the first minutes under heat. Nevertheless, no furan protons were consumed during the reaction while the double bond of MI fully disappeared after 180 min (*Figure 2 a*)) indicating that Diels-Alder reaction did not occur. Maleimide double bond was consumed by aza-Michael addition instead (*Scheme 1* c)). Indeed, the free amines of chitosan might react with the double bond of maleimide. The same experiment was reproduced in D_2O with 1 % and 2 % of acetic acid (*Figure 2 b)*). In this solvent, furan and maleimide were both consumed during the reaction to form the Diels-Alder adduct in acid media (1 and 2%) (*Scheme 1* d)). Indeed, free amines of FGO are protonated thus hindering their nucleophilic attack onto MI by Michael addition. By performing the reaction in DMSO with 1% of acetic acid, Michael reaction did not occur, confirming this assumption. Thus, the reaction conditions were set as follows: chitosan was dissolved in 2% acetic acid solution to facilitate the dissolution of the high molar mass chitosan CH150 then the maleimides BMI and TMI were added after dissolution in a minimum amount of DMSO (250 µL).

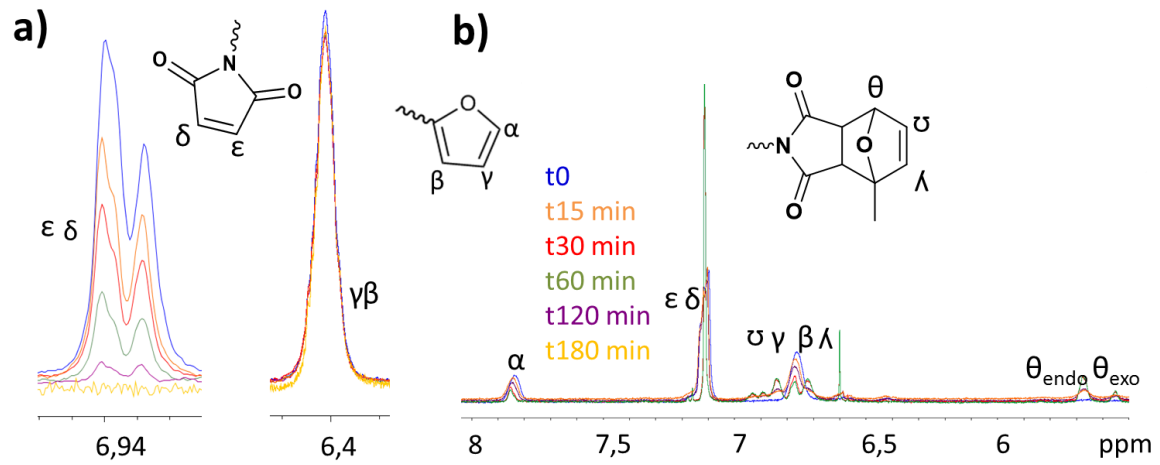

Figure 2. a) Following of ^{1}H NMR monitoring of FGO+MI at 65 °C in DMSO for 180 min b) Following ^{1}H NMR of FGO + excess of MI in D_2O, 1% AcOH for 180 min

3.3.2. Reaction between MI and CH30FG

To confirm that the reaction occurs on higher molar masses, it was reproduced with CH30FG and MI. It was shown by ^{1}H NMR spectroscopy (*Figure 3c*) that the Diels-Alder adducts (endo and exo forms) were produced with the appearance of peaks between 6.3 and 6.7 ppm as well as 5.2 ppm corresponding to the endo adduct (55%) and at 5 ppm for the exo form (45%). Moreover, the decrease of the furan signal intensities at 6.5 ppm and 7.6 ppm was also observed. Nevertheless, the reaction did not proceed quantitatively, as 10% of unreacted furan groups still remained after 24 h despite the use of 1 eq of MI (*Figure 3*). However, it was shown by IR spectroscopy that there was no residual unreacted maleimide. This could be explained from the DS calculation based on acetylation degree or from side Michael addition.

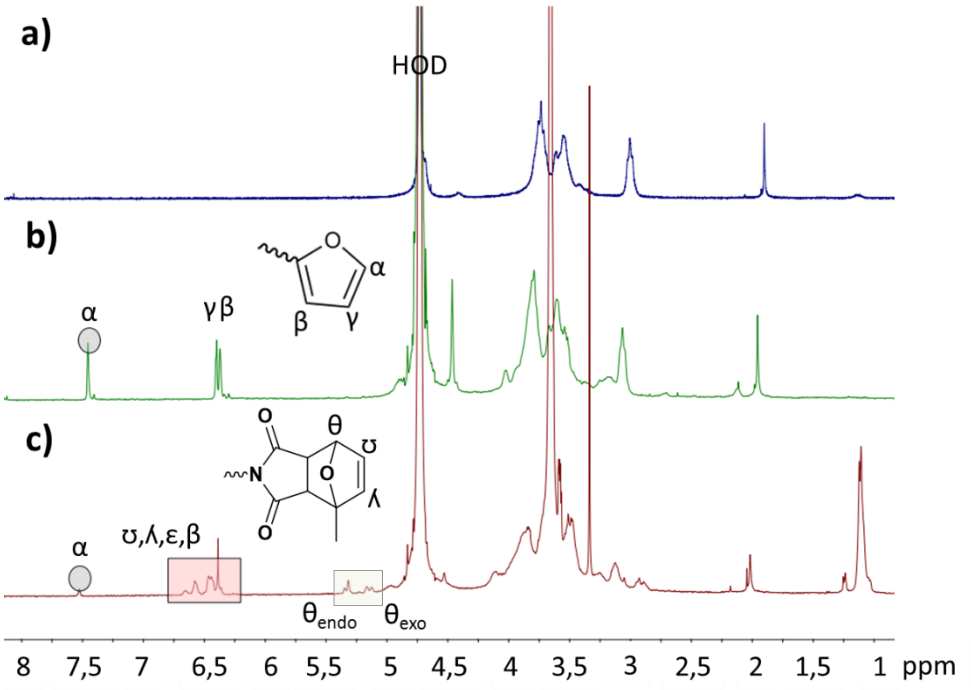

Figure 3. a) ^{1}H NMR of CH30 in D_2O+TFA b) ^{1}H NMR of CH30FG in D_2O+TFA c) ^{1}H NMR of CH30FGMI in D_2O+TFA

The resulting product from the reaction of MI and CH30FG was analyzed by DSC, a common method to determine if the retro Diels-Alder reaction occurred (Dolci et al., 2015). The thermogram of CH30FGMI exhibited a complex endothermic peak starting at 110 °C with a first peak at 117 °C and a second one at 128 °C both corresponding to the retro Diels-Alder reaction for *endo* and *exo* adducts respectively (Froidevaux et al., 2015). Moreover, the enthalpy of the retro Diels-Alder reaction was measured (-15.88 J/g) and similar to the value from literature (-18.09 J/g) with *endo* peak at 128 °C and *exo* peak at 157 °C (Duval et al., 2017) (*Figure 4*).

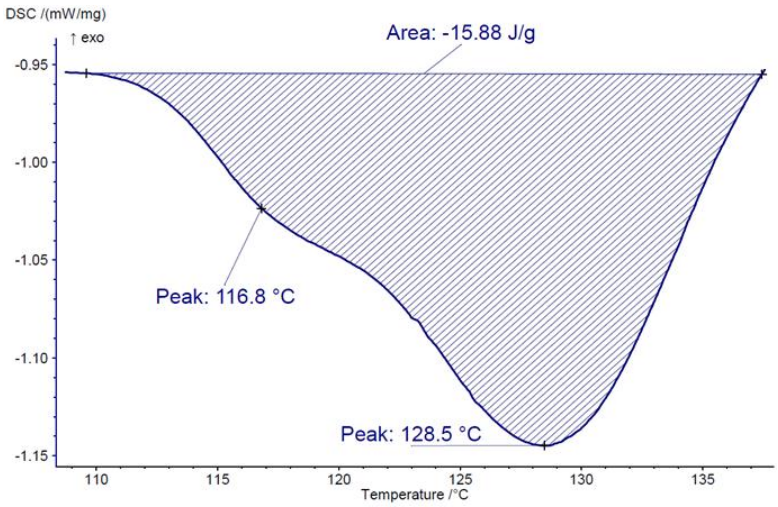

Figure 4. DSC measurement of CH30MI

After DSC analysis, the sample was recovered and characterized by ^{1}H NMR. It confirmed that the retro Diels-Alder occurred as the peaks at 6.5 ppm and 7.6 ppm corresponding to furan were recovered when peaks between 6.3 and 6.7 ppm corresponding to the Diels-Alder adduct disappeared (see SI 3). Many studies have been performed on cross-linked chitosan systems using the Diels-Alder reaction, but the retro Diels-Alder was never considered in those studies. Hence, to our knowledge our present study is the first one to highlight by structural and thermal analyses the retro Diels-Alder reaction for such polysaccharide systems.

3.4. Films making and characterizations

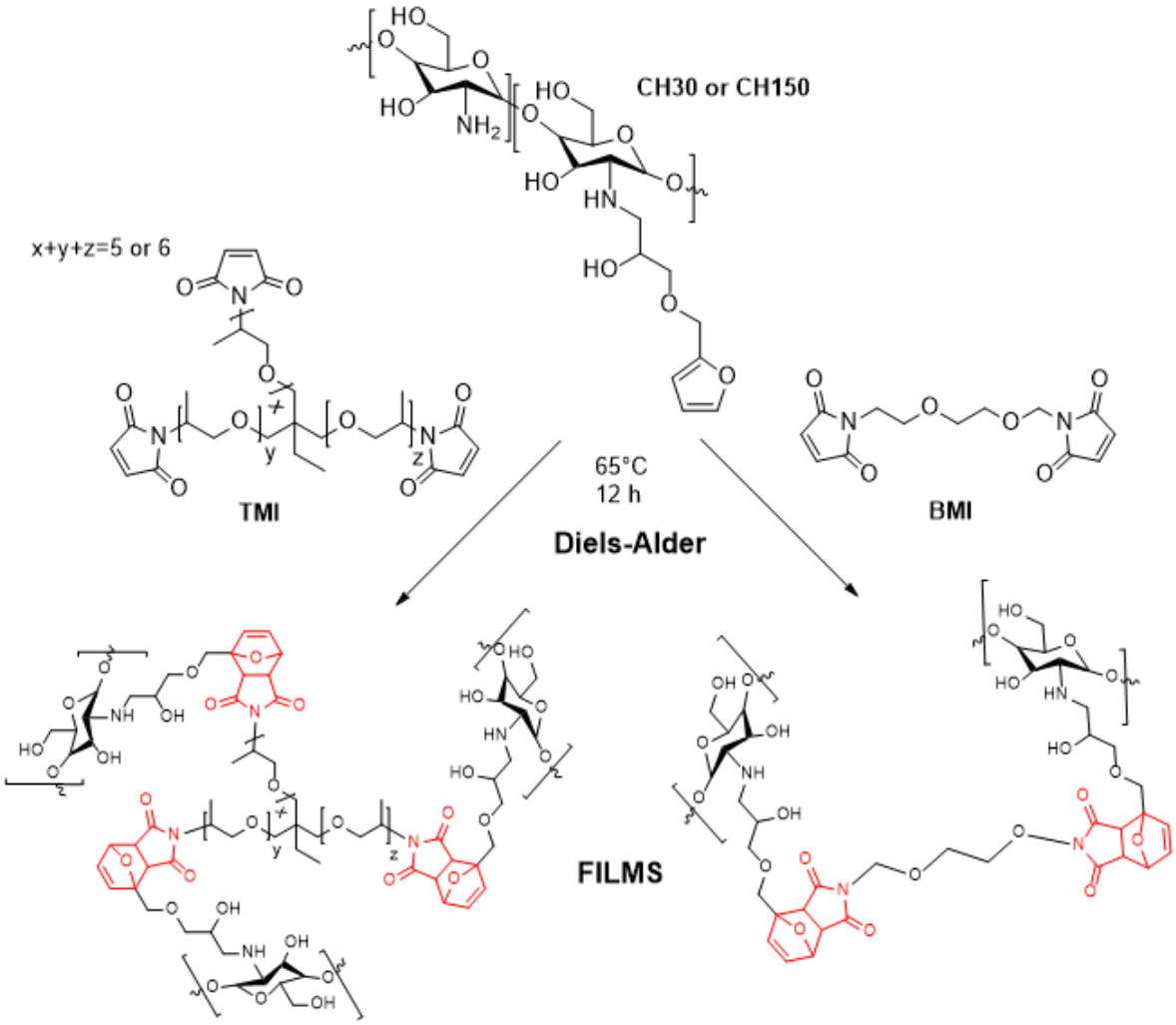

Scheme 2. Synthesis of chitosan-furan based films by Diels-Alder click chemistry with dis and tris-maleimide cross-linkers.

After dissolution of the furan modified-chitosan in 2% acetic acid solution with a concentration of 1 wt% for CH30 and 0.5 wt% for CH150, the maleimides i.e. BMI or TMI dissolved in 250 µL of DMSO, were added. For homogenizing, the solution was then mixed using a speed mixer for 3 min at 2500 rpm. The solution was then deposited on a PTFE- glass films (thickness: 0.23 mm) and allowed to react during 12 h in an oven at 65 °C.

Sample	Contact angle (°)	*Swelling ratio at 24 h at pH 4 (%)*	*Swelling ratio at 24 h in PBS pH 7.4 0.1 M (%)*	*E' at 25 °C (GPa)*
CH30	90 ± 4	N/A	335	5.10^{-2}
CH30BMI	107 ± 10	235	174	1.8
CH30TMI	99 ± 6	232	230	5.2
CH150	N/A	N/A	557	N/A
CH150BMI	120 ± 3	344	220	6.0
CH150TMI	118 ± 5	450	280	4.8

Table 1. Contact angle, swelling ratio at different pH and E' of CH30 and CH150 films

The films were then analysed by infrared spectroscopy to demonstrate the reactivity between the maleimide crosslinkers and the furan groups from chitosan to form a network. Indeed, a significant signal at 820 cm^{-1} was attributed to the double bond of maleimide and a signal at 875 cm^{-1} to the double bond of furan from the starting reagents according to *Figure 5*. Both double bonds were consumed during the reaction as the signals no longer appeared in BMI films (*Figure 5* c)). As for the model study using MI, it displayed a complete conversion of the maleimide BMI or TMI in the presence of CH30FG or CH150FG

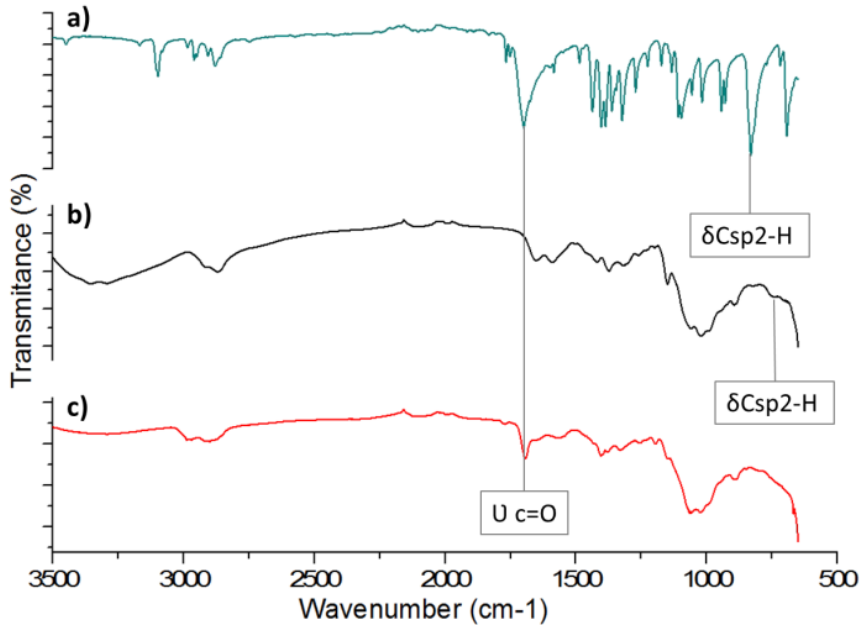

Figure 5. a) Infrared spectrum of BMI b) Infrared spectrum of CH30FG film c) Infrared spectrum of CH30FG-BMI film

3.4.1. Thermo-mechanical properties

Usually, mechanical properties of chitosan films are characterized by tensile strength analyses (Hou et al., 2020), (Ren et al., 2017). However, as we previously highlighted the retro Diels-Alder reaction on CH30MI by DSC, dynamic mechanical analyses (DMA) was a promising technique to assess the occurrence of the retro Diels-Alder reaction on our cross-linked chitosan films. Therefore, thermo-dynamical properties of chitosan films have been studied with DMA, storage modulus (E') at room temperature are summarized in *Table 1* and a magnification from 45 °C to 190 °C of the analyses is shown in *Figure 6*. In order to perform DMA analyses, homogeneous films were prepared. No homogeneous films were obtained for the crude CH150. However, once crosslinked with BMI and TMI, homogeneous films were provided and were further analysed. CH30 films were homogeneous either crude or in combination with a maleimide compound. The DMA analysis of CH30 showed a stable E' (50 MPa) over the whole temperature range. CH30BMI, CH30TMI films were much stiffer due to their Diels-Alder cross-linking, with an increase of E' of orders of magnitude of one hundred. Due to the higher functionality of TMI, CH30TMI is stiffer than CH30BMI as TMI may induce a higher cross-link density. Concerning CH150BMI and CH150TMI, the

entanglements of 150,000 g/mol chitosan chains was assumed to lower the cross-linker effect. Thanks to the Diels-Alder cross-linking, E' value of CH30TMI film was rather similar to CH150BMI and CH150TMI. This cross-linking is therefore a good alternative to obtain high mechanical properties from low molar mass chitosan. DMA analyses involved a temperature increase and as we demonstrated previously with CH30FGMI, retro Diels-Alder reaction occurs at 117 °C and 128 °C. As shown in *Figure 6*, cross-linked films did not show a stable E' compared to CH30. At around 100 °C, E' value of the four cross-linked films started to drop. This fluctuation may be induced by the retro Diels-Alder reaction. Indeed, during this reaction the cross-linking density dropped because cross-linking nodes were destroyed, the network destruction inducing a decrease of E' value. Those dynamical analyses allowed demonstrating the interest of cross-linked chitosan films. Thanks to the cross-linking step, homogeneous films of CH150BMI and CH150TMI were obtained, low molar mass CH30BMI and CH30TMI films showed mechanical properties comparable to high molar mass chitosan films. Moreover, we were the first to our knowledge to characterize chitosan films by DMA and to highlight the retro Diels-Alder reaction at high temperature (117°C and 128°C) on cross-linked chitosan films.

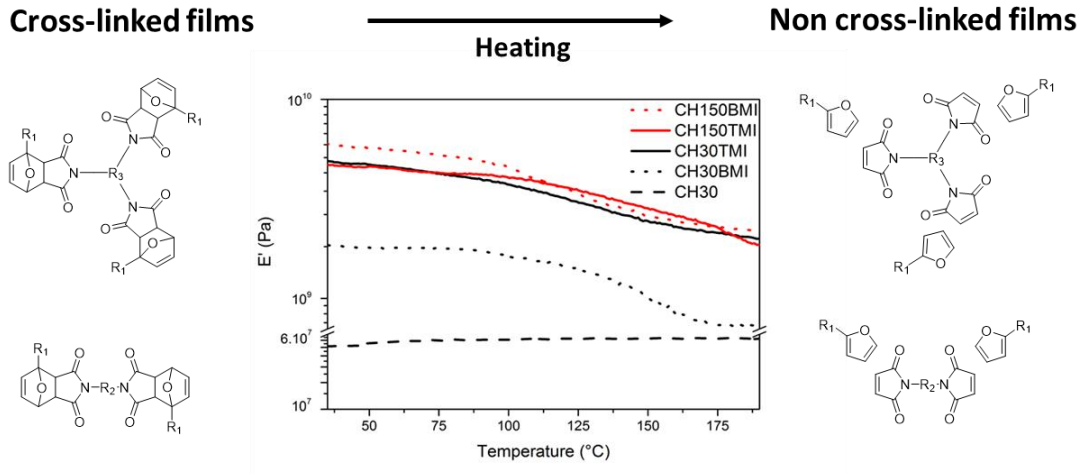

Figure 6. DMA measurements of chitosan films (R_1: chitosan chain; R_2: PEG chain; R_3 PPG chain)

3.4.2. Swelling index at different pH

The swelling capacity of chitosan films was studied at pH 7.4 and pH 4. ***Erreur ! Référence non valide pour un signet.*** shows the swelling index of cross-linked and non-cross-linked films over 24 h. First, swelling index of films was measured in PBS at pH 7.4. When cross-linked with BMI, CH30BMI and CH150BMI showed the lower swelling index, 174% and 220% respectively. Films cross-linked with TMI had slightly higher swelling index with 230% and 280% for CH30TMI and CH150TMI respectively. . It could be assumed that the cross-link density was higher using BMI although its lower functionality indeed, its low size in comparison to TMI chains led to closer cross-linking nodes, therefore BMI films swelled less. For non-cross-linked films, higher molar mass chitosan led to higher swelling index, 335% and 557% for CH30 and CH150 respectively. However, this difference was lowered once films were cross-linked. On the other hand, film swelling capacity was measured at pH 4 where chitosan is fully soluble, especially low molar masses. Indeed, CH30 and CH150 were soluble in these conditions and the swelling index could not be measured, the films were not recovered after their addition in the acidic solution. However, the four others CH30BMI, CH30TMI, CH150BMI and CH150TMI were not soluble, confirming their cross-linking. In the same way as in PBS, CH30TMI and CH150TMI had slightly higher swelling index than their BMI equivalents. Due to electrostatic repulsion of amino groups of chitosan chains, at pH 4 amines are charged and their repulsion leads to higher swelling index. However, once chitosan chains are cross-linked, their electrostatic repulsion is highly reduced, keeping a swelling index almost similar at pH 7.4 and pH 4.

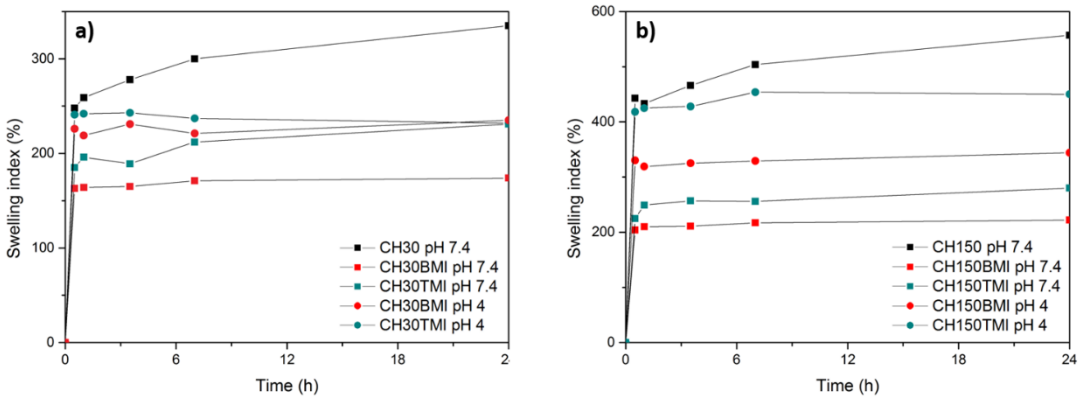

Figure 7. Swelling index of chitosan films over time at pH 4 and pH 7.4 a) films from CH30 b) films from CH150

3.4.3. Contact angle

Contact angle between water and films were determined *(Table 1*). For crude CH30, contact angle was in accordance with the literature (Luo et al., 2014). It was shown that cross-linked films have higher hydrophobicity compared to net chitosan films, especially for crude CH150 for which the film was not homogeneous and it was difficult to measure an angle as the drop was directly absorbed (SI 3). Once again, this analysis confirmed that the crosslinking occurred. It was also shown that once cross-linked, the higher are the molar masses, the higher is the contact angle which is in accordance with the chitosan properties. Contact angle between hexadecane and films was also experimented. It was shown that for any film, the drop was immediately absorbed and no angle could be measured. It meant that chitosan films, crosslinked or not, could absorb fatty component as chitosan is well known for being a fat binder (Raval et al., 2017).

All those combined properties could open the way for many application in food packaging for example with the well-known antioxidant properties of chitosan (Kabanov & Novinyuk, 2020)' (Elsabee & Abdou, 2013) . The proof of concept of the reversible Diels-Alder reaction also opens the way to new types of cross-linkers. Indeed, it could be imagined to use other bis or trimaleimide and even other aromatic compounds, to tune the properties of the film,

perhaps making thermoreversible hydrogels as described previously (Montiel-Herrera et al., 2015).

4. Conclusions

In this work, a model study was carried out on Diels-Alder and retro Diels-Alder reaction between maleimide moieties and furan functionalized chitosan. Both reactions were evidenced for the first time by NMR spectroscopy and the retro Diels Alder temperatures were determined by DSC for non-reticulated products. In the meantime, different films were prepared from the chitosan modified with pending furan and maleimide cross-linker. It was shown that efficient crosslinking through Diels Alder chemistry occurred at 65°C. The retro Diels-Alder was also evidenced for the first time in chitosan systems and to occur between 110 and 130 °C. Finally, thanks to the cross-linking, homogeneous films were obtained. It was shown that higher crosslinking density played a more important role than the chitosan molar mass in the resulting mechanical properties, with better properties for TMI based films. Crosslinked films also showed fat absorption and higher hydrophobicity than chitosan alone, which could be promising materials for bio-based coatings applications.

5. Associated content

Appendix A supplementary data.

Copies of ^{13}C spectra, FT-IR, ^{1}H NMR for the compounds of interest and contact angles pictures of the various films.

Abbreviations

FG: furfuryl glycidyl ether

BMI: bismaleimide

TMI: trimaleimide

DS: Substitution degree

DA: acetylation degree

6. Author information

Corresponding author

*Email: ghislain.david @enscm.fr

Tel: +33 0467144307/0660335363

Address : current address

Notes

The authors declare no competing financial interest.

7. Acknowledgements

The authors would like to thanks Lucie Grossenbacher for her help in the project, Christine Joly-Duhamel for her advices and Cedric Totee for the NMR analysis.

8. References

Chapelle, C., David, G., Caillol, S., Negrell, C., Durand, G., Desroches Le Foll, M., & Trombotto, S. (2019). Water-Soluble 2,5-Anhydro- d -mannofuranose Chain End Chitosan Oligomers of a Very Low Molecular Weight: Synthesis and Characterization. *Biomacromolecules*, *20*(12), 4353–4360. https://doi.org/10.1021/acs.biomac.9b01003

Divya Nataraj, Seema Sakkara, M. M. N. (2018). Crosslinked chitosanfilms with controllable properties for comercial applications.pdf. *International Journal of BiologicalMacromolecules*, *120*, 1256–1264.

Dolci, E., Michaud, G., Simon, F., Boutevin, B., Fouquay, S., & Caillol, S. (2015). Remendable thermosetting polymers for isocyanate-free adhesives: A preliminary study. *Polymer Chemistry*, *6*(45), 7851–7861. https://doi.org/10.1039/c5py01213a

Dragan, E. S., & Dinu, M. V. (2019). Polysaccharides constructed hydrogels as vehicles for proteins and peptides . A review. *Carbohydrate Polymers*, *225*(August), 115210. https://doi.org/10.1016/j.carbpol.2019.115210

Duval, A., Couture, G., Caillol, S., & Avérous, L. (2017). Biobased and Aromatic Reversible Thermoset Networks from Condensed Tannins via the Diels-Alder Reaction. *ACS Sustainable Chemistry and Engineering*, *5*(1), 1199–1207. https://doi.org/10.1021/acssuschemeng.6b02596

Elsabee, M. Z., & Abdou, E. S. (2013). Chitosan based edible fi lms and coatings : A review. *Materials Science & Engineering C*, *33*(4), 1819–1841. https://doi.org/10.1016/j.msec.2013.01.010

Elschner, T., Obst, F., & Heinze, T. (2018). Furfuryl- and Maleimido Polysaccharides: Synthetic Strategies Toward Functional Biomaterials. *Macromolecular Bioscience*, *18*(11). https://doi.org/10.1002/mabi.201800258

Froidevaux, V., Borne, M., Laborbe, E., Auvergne, R., Gandini, A., & Boutevin, B. (2015). Study of the diels-alder and retro-diels-alder reaction between furan derivatives and maleimide for the creation of new materials. *RSC Advances*, *5*(47), 37742–37754.

https://doi.org/10.1039/c5ra01185j

Gandini, A., Carvalho, A. J. F., Trovatti, E., Kramer, R. K., & Lacerda, T. M. (2018). Macromolecular materials based on the application of the Diels–Alder reaction to natural polymers and plant oils. *European Journal of Lipid Science and Technology*, *120*(1), 1–20. https://doi.org/10.1002/ejlt.201700091

García-astrain, C., Hernández, R., Guaresti, O., Fruk, L., Mijangos, C., Eceiza, A., & Gabilondo, N. (n.d.). *Click Crosslinked Chitosan / Gold Nanocomposite Hydrogels*. 1295–1300.

Gregorio Crini , Pierre-Marie Badot, E. G. (n.d.). *Chitine et Chitosane Du biopolymère à l'application*.

Guaresti, O., García-Astrain, C., Aguirresarobe, R. H., Eceiza, A., & Gabilondo, N. (2018). Synthesis of stimuli–responsive chitosan–based hydrogels by Diels–Alder cross–linking `click´ reaction as potential carriers for drug administration. *Carbohydrate Polymers*, *183*(December 2017), 278–286. https://doi.org/10.1016/j.carbpol.2017.12.034

Guaresti, O., Garcia-Astrain, C., Urbina, L., Eceiza, A., & Gabilondo, N. (2019). Reversible swelling behaviour of Diels–Alder clicked chitosan hydrogels in response to pH changes. *Express Polymer Letters*, *13*(1), 27–36. https://doi.org/10.3144/expresspolymlett.2019.4

Guaresti, O., García–Astrain, C., Palomares, T., Alonso–Varona, A., Eceiza, A., & Gabilondo, N. (2017). Synthesis and characterization of a biocompatible chitosan–based hydrogel cross–linked via 'click' chemistry for controlled drug release. *International Journal of Biological Macromolecules*, *102*, 1–9. https://doi.org/10.1016/j.ijbiomac.2017.04.003

Hamedi, H., Moradi, S., Hudson, S. M., & Tonelli, A. E. (2018). Chitosan based hydrogels and their applications for drug delivery in wound dressings : A review. *Carbohydrate Polymers*, *199*(March), 445–460. https://doi.org/10.1016/j.carbpol.2018.06.114

Hou, C., Gao, L., Wang, Z., Rao, W., Du, M., & Zhang, D. (2020). Mechanical properties, thermal stability, and solubility of sheep bone collagen–chitosan films. *Journal of Food Process Engineering*, *43*(1), 1–8. https://doi.org/10.1111/jfpe.13086

Jin, J., Song, M., & Hourston, D. J. (2004). Novel Chitosan-Based Films Cross-Linked by Genipin with Improved Physical Properties. *Biomacromolecules*, *5*, 162–168. https://doi.org/10.1021/bm034286m

Kabanov, V. L., & Novinyuk, L. V. (2020). Chitosan Application in Food Technology: a Review of Rescent Advances. *Food Systems*, *3*(1), 10–15. https://doi.org/10.21323/2618-9771-2020-3-1-10-15

Kavianinia, I., Plieger, P. G., Kandile, G., & Rk, D. (2014). Preparation and characterization of chitosan films , crosslinked with symmetric aromatic dianhydrides to achieve enhanced thermal properties. *Polym Int*, *64*, 556–562. https://doi.org/10.1002/pi.4835

Kaya, M., Khadem, S., Cakmak, S., & Mujtaba, M. (2018). Antioxidative and antimicrobial edible chitosan films blended with stem, leaf and seed extracts of Pistacia terebinthus for active food packaging. *RSC Advances*, *8*, 3941–3950. https://doi.org/10.1039/c7ra12070b

Liu, J., Meng, C., Liu, S., Kan, J., & Jin, C. (2017). Food Hydrocolloids Preparation and characterization of protocatechuic acid grafted chitosan fi lms with antioxidant activity. *Food Hydrocolloids*, *63*, 457–466. https://doi.org/10.1016/j.foodhyd.2016.09.035

Luo, Y., Pan, X., Ling, Y., Wang, X., & Sun, R. (2014). Facile fabrication of chitosan active film with xylan via direct immersion. *Cellulose*, *21*(3), 1873–1883. https://doi.org/10.1007/s10570-013-0156-4

Matsumoto, M., Udomsinprasert, W., Laengee, P., Honsawek, S., Patarakul, K., & Chirachanchai, S. (2016). A Water-Based Chitosan-Maleimide Precursor for Bioconjugation: An Example of a Rapid Pathway for an In Situ Injectable Adhesive Gel. *Macromolecular Rapid Communications*, *37*(19), 1618–1622. https://doi.org/10.1002/marc.201600257

Montiel-Herrera, M., Gandini, A., Goycoolea, F. M., Jacobsen, N. E., Lizardi-Mendoza, J., Recillas-Mota, M., & Argüelles-Monal, W. M. (2015). N -(furfural) chitosan hydrogels based on Diels–Alder cycloadditions and application as microspheres for controlled drug release. *Carbohydrate Polymers*, *128*, 220–227. https://doi.org/10.1016/j.carbpol.2015.03.052

Montiel, M., Alessandro, H., Francisco, G., Jacobsen, N. E., Lizardi, J., Maricarmen, M., Mota, T. R., & Monal, W. M. A. (2015). Furan – chitosan hydrogels based on click chemistry. *Iranian Polymer Journal*, 349–357. https://doi.org/10.1007/s13726-015-0325-4

Na, H. N., Park, S. H., Kim, K. Il, Kim, M. K., & Son, T. Il. (2012). Photocurable O-carboxymethyl chitosan derivatives for biomedical applications: Synthesis, in vitro biocompatibility, and their wound healing effects. *Macromolecular Research*, *20*(11), 1144–1149. https://doi.org/10.1007/s13233-012-0167-2

Pakdel, P. M., & Peighambardoust, S. J. (2018). Review on recent progress in chitosan-based hydrogels for wastewater treatment application. *Carbohydrate Polymers*, *201*(August), 264–279. https://doi.org/10.1016/j.carbpol.2018.08.070

Raval, R., Rangnekar, R. H., & Raval, K. (2017). Optimization of Chitosan Nanoparticles Synthesis and Its Applications in Fatty Acid Absorption. *Materials, Energy and Environment Engineering*, 253–256. https://doi.org/10.1007/978-981-10-2675-1

Ren, L., Yan, X., Zhou, J., Tong, J., & Su, X. (2017). Influence of chitosan concentration on mechanical and barrier properties of corn starch/chitosan films. *International Journal of Biological Macromolecules*, *105*, 1636–1643. https://doi.org/10.1016/j.ijbiomac.2017.02.008

S. Bhuvaneshwari *, D.Sruthi*, V. Sivasubramanian*, N. kalyani** and J. S. **. (2014). Development and characterization of chitosan film.pdf. *International Journal of Engineering Research and Applications (IJERA)*, *1*(2), 292–299.

Singh, Kuldeep Rajat Suri, A. K. T., & Rana, V. (2012). Chitosan films crosslinking with EDTA modifies physicochemical.pdf. *Mater Sci: Mater Med*, *23*, 687–695.

Tiwary, A. K., & Rana, V. (2010). Cross-linked chitosan films : Effect of cross-linking density on swelling parameters. *Pak. J. Pharm. Sci.*, *May 2014*, 443–448.

Vauthier, M., Jierry, L., Oliveira, J. C., Hassouna, L., Roucoules, V., & Bally-Le Gall, F. (2019). Interfacial Thermoreversible Chemistry on Functional Coatings: A Focus on the Diels–Alder Reaction. *Advanced Functional Materials*, *29*(10), 1–16. https://doi.org/10.1002/adfm.201806765

Y.X. Xua, K.M. Kimb, M.A. Hannaa,∗, D. N. (2005). Chitosan–starch composite film preparation.pdf. *Industrial Crops and Products*, *21*, 185–192.

Yang, S., Du, X., Deng, S., Qiu, J., Du, Z., Cheng, X., & Wang, H. (2020). Recyclable and self-healing polyurethane composites based on Diels-Alder reaction for efficient solar-to-thermal energy storage. *Chemical Engineering Journal*, *398*(February), 125654. https://doi.org/10.1016/j.cej.2020.125654

Zhang, M., Wang, J., & Jin, Z. (2018). Supramolecular hydrogel formation between chitosan and hydroxypropyl β-cyclodextrin via Diels-Alder reaction and its drug delivery. *International Journal of Biological Macromolecules*, *114*, 381–391. https://doi.org/10.1016/j.ijbiomac.2018.03.106